CFD-Enabled Optimization of Polymerase Chain Reaction Thermal Flow Systems

Hazim S. Hamad [1✉,2]

Email mnhsh@leeds.ac.uk

N. Kapur [1]

Z. Khatir [3]

Osvaldo Querin [1]

H. M. Thompson [1]

M. C. T. Wilson [1]

[1] School of Mechanical Engineering, University of Leeds, Leeds, UK

[2] Ministry of Oil, Baghdad, Iraq

[3] School of Engineering and the Built Environment, Birmingham City University, Birmingham, B4 7XG, UK

Abstract

The abstract is published online only. If you did not include a short abstract for the online version when you submitted the manuscript, the first paragraph or the first 10 lines of the chapter will be displayed here. If possible, please provide us with an informative abstract.

Microfluidic flow systems with precise thermal control are required in many important practical applications, such as in heat sink cooling of electronics, droplet freezing systems to determine environmental pollution levels and in efficient chemical processing [1, 2, 3]. This study focuses on the thermal microfluidic flows arising in Polymerase Chain Reaction (PCR) thermal cycling systems used for rapid diagnostic screening and testing [4]. PCR systems have been widely studied and numerous design features have been proposed to regulate the temperature distribution to provide the required thermal environment for effective amplification of DNA needed to complete the process [3]. Microfluidics are very useful for such systems since they can

reduce the reagent consumption and the thermal mass, which enables the temperature to be manipulated rapidly within the various temperature zones needed for the denaturation, annealing, and extension components of the PCR process. Computational Fluid Dynamics is used to explore the effect of microfluidic geometry and operating conditions on the thermal and hydraulic conditions within each of the three temperature zones. The COMSOL Multiphysics® 5.4 coupled with MATLAB codes are used to solve a novel series of optimization problems that enable the most effective thermal conditions for the process of DNA amplification to be identified. The study focuses on a prototype serpentine microfluidic geometry that enables multiple cycles of denaturation, annealing, and extension to be carried out within a single microfluidic chip. Using accurate meta-modelling and stochastic optimization methods, the first time single optimization study is determined that enabled a series of Pareto fronts to determine compromises that can be struck between the competing multiple objectives in PCR systems.

1. Introduction

The polymerase chain reaction (PCR) is a significant technique used to make thousands to millions of copies of particular DNA, and involves a process of heating and cooling called thermal cycling which can be conducted by a PCR device. The PCR process requires exposing the sample to different temperature zones which are denaturation (95 °C), annealing (54 °C), and extension (72 °C) [5]. These three temperature levels are essential in the PCR reaction, and this process is considered to have failed in the absence of one of these cycles. The conventional PCR that is commercially available consists of 96 wells containing the reagent mixture and DNA sample [6]. The thermal cycle of this type of PCR is controlled by liquid or air circulation to heat up and cool down the overall chamber in order to achieve the PCR steps, so this results in large thermal mass and is time-consuming (about 1−2 h) and requires high power consumption [6, 7]. Recently, with advances in the field of miniaturization and microelectromechanical systems (MEMS) technology, which has been used to fabricate microfluidic devices [8], the trend has changed from macro-PCR to microfluidic-based PCR, which offers several advantages including smaller sample volumes, total reaction times, and power and material consumption [6, 8]. Micro-PCR based on a stationary reaction chamber made of silicon was first developed in 1993 by Northrup [9], in which a fast and efficient PCR compared to conventional PCR was obtained. The design of micro-PCR was improved to perform continuous flow polymerase chain reaction (CFPCR) [10], which dramatically shortened PCR process times [11]. The CFPCR process is achieved by cycling the PCR mixture through three PCR zones to achieve the desired

temperature instead of heating and cooling all the entire chip. Therefore, the heating and energy consumption are reduced and the thermal cycles could be achieved faster than in a stationary PCR-based chamber [12]. A CFPCR channel was first presented by Kopp et al. [12] in 1998 who designed serpentine cyclic identical channels etched on a glass chip and equipped with an independent copper block to support temperature uniformity. In addition, a temperature gradient technique was employed to simplify the process of creating the desired temperature zones. Crews et al. [13] presented channels with thirty and forty serpentine PCR cycles, made of glass and heated and cooled by two thermal aluminum strips placed underneath. A comparison between DNA amplification results with commercial macroscale devices was achieved and the amplification time of control samples was 10 min for the 30-cycle PCR and 13 min for the 40-cycle PCR. Moschou et al. [14] presented thirty serpentine cycle channels made of polyimide with relative time ratios of 1:1:2 for denaturation, annealing, and extension, respectively, and three integrated resistive copper heaters as heating elements. They achieved efficient DNA amplification within 5 min. Schneegaß et al. [15] fabricated a 25 cycle PCR device made of silicon and glass. The device consisted of reaction chambers etched into a glass chip and covered by a silicon chip and equipped with heaters. They obtained residence times of a sample volume for the 25 cycle device of approximately 25 min, and the energy consumption was 0.012 kWh for a 35 min of the PCR process. Hashimoto et al. [16] presented a 20-cycle microchannel in a spiral shape made of polycarbonate to study and evaluate the effect of high velocity on thermal and biochemical characteristics in CFPCR. Zhang et al. [17] used ANSYS Fluent to optimize the effect of different material on CFPCR chip design, but the flow effect was neglected. Chen et al. [18] presented an analytical study to investigate the influence of geometrical chip parameters and various chip materials on temperature uniformity with no flow condition.

AQ1

Previous studies have focused on comparatively small fluidic PCR channels in order to achieve the desired temperature by decreasing the effect of convection, albeit with larger pressure drop. A number of questions regarding the relationships among residence time, heating power, and pressure drop and temperature uniformity still need to be addressed. Since there is a wide design space in terms of geometrical, flow, and thermal parameters, and important constraints on the process, research in microfluidic PCR systems could greatly benefit from the multi-objective optimization studies. With this motivation, this paper aims to use CFD-based optimization to investigate the effect of microfluidic geometry and operating conditions on the effectiveness of PCR design within each of the three temperature zones.

2. PCR Design

The CFPCR chip under consideration has been designed based on a single microfluidic channel etched on glass for its low thermal conductivity, bounded by a PMMA cover for its low cost and good optical access and three copper blocks with cartridge heaters placed underneath the glass chip. The microfluidic channel passes through isothermal temperature regions as shown in Fig. 1. Water has been chosen as the working fluid, the inlet temperature is 20 °C, and the Reynolds number is fixed at 0.7 and the outside wall is assumed to be insulated. Moreover, the bottom of the copper heaters was set at 95 °C, 72 °C, and 56 °C, respectively, and the distance between heaters S is kept constant 1.5 mm, the length of heater (L_h) at each zone is 9 mm, and the height of the heater H_h (100 μm). The schematic diagram of the channel geometry is described in Fig. 2 where W_c(μm), H_c (μm), W_w (μm), H_b (μm), L (mm) are, respectively, the microchannel width, height, the wall thickness W_w μm, the bottom height, and the length.

Fig. 1

PCR process and design

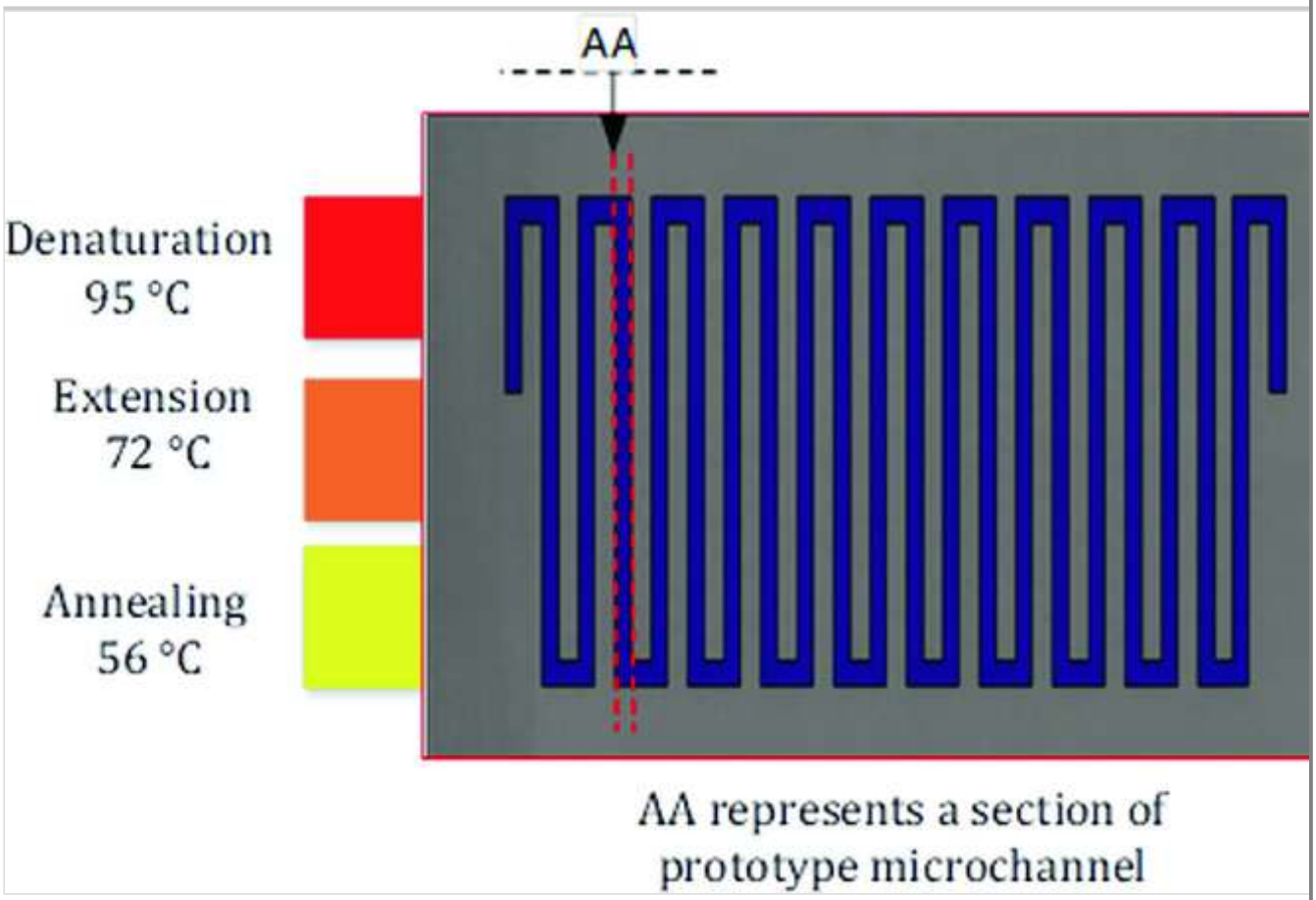

Fig. 2

Schematic diagram of microfluidic channel

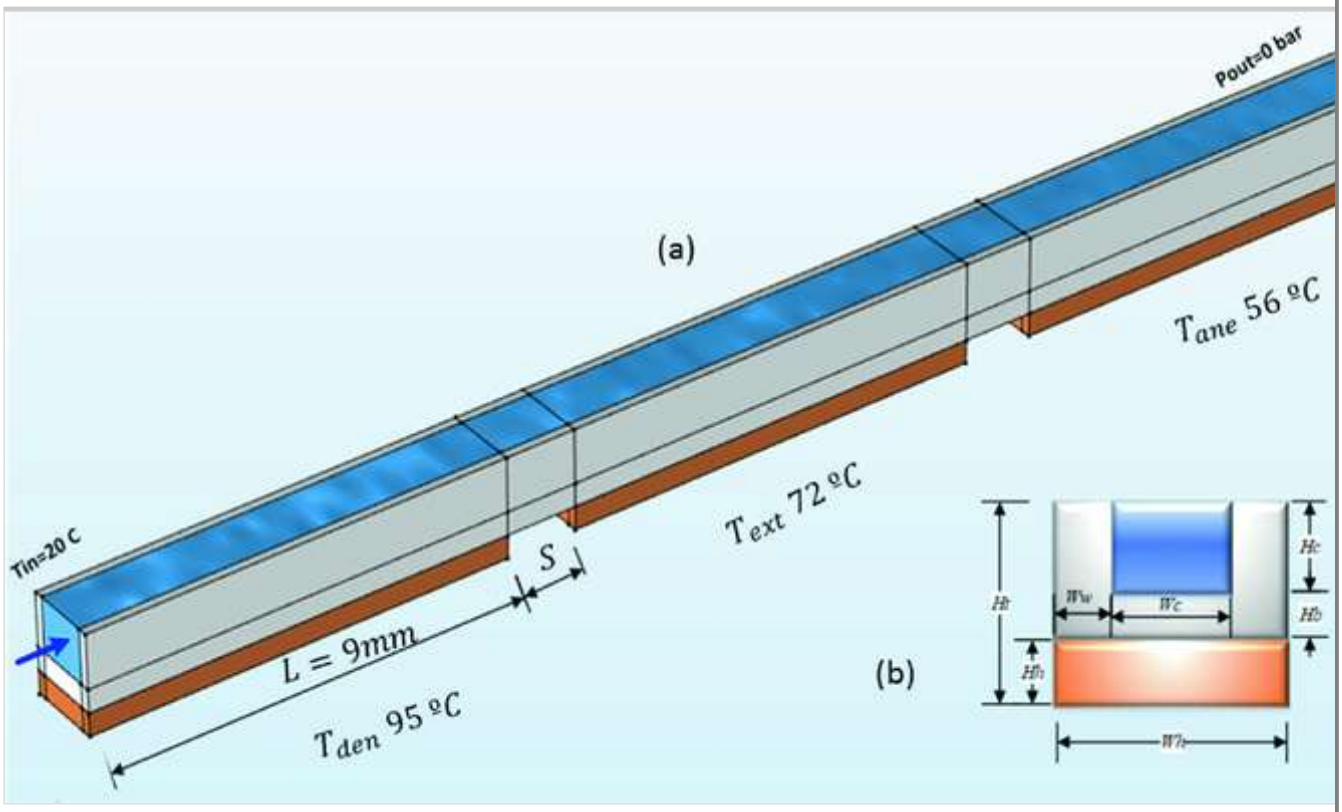

3. Modeling

Steady state, three-dimensional single-phase water flow and heat transfer in the microchannel PCR is modelled using the governing Eqs. (1)–(4), comprising the continuity and Navier-Stokes equations together with the energy equations for the liquid and solid:

$$\nabla \cdot (\rho \boldsymbol{u}) = 0 \text{ (continuity equation)} \tag{1}$$

$$\rho_f (\mathbf{u} \cdot \nabla \mathbf{u}) = -\nabla p + \mu \nabla^2 \mathbf{u} \quad \text{(momentum equation)} \tag{2}$$

$$\rho_{\mathrm{f}} C_{\mathrm{pf}} (\mathbf{u} \cdot \nabla T) = k_{\mathrm{f}} \nabla^2 T \quad \text{(Heat transfer (energy) equation for the liquid)} \tag{3}$$

$$k_{\mathrm{s}} \nabla^2 T_{\mathrm{s}} = 0 \quad \text{(Heat transfer (energy) equation for the solid)} \tag{4}$$

where u and p are the fluid velocity vector [m/s] and the fluid pressure (Pa), respectively, and C_{pf}, ρ_{f}, k_{f}, and k_{s} represent the specific heat, density, and thermal conductivity of the fluid and thermal conductivity of the solid,

respectively. COMSOL Multiphysics® version 5.4 is used to solve this conjugate heat transfer model by assuming the fluid flow to be incompressible, Newtonian, and laminar. Radiative heat transfer is neglected, and there are no internal heat sources.

4. Numerical Validation

The numerical model has been validated by comparison with the numerical results of Toh et al. [19] and experimental results of Tuckerman [20]. For the purpose of this comparison, the constant-temperature boundary condition and Reynolds number were replaced with a heat flux $q\,(\mathrm{W/cm^2})$ and a volumetric flow rate $\dot{V}\,(\mathrm{cm^3/s})$ and it showed a good agreement with available numerical and experimental results as listed in Table 1.

Table 1

Thermal resistances validation of the present work against Tuckerman [20] experimental work, and numerical data of Toh et al. [19]

Case	$q\left(\mathrm{W/cm^2}\right)$	$\dot{V}\left(\mathrm{cm^3/s}\right)$	$R_{\mathrm{th}}\ (\mathrm{cm^2\,K/W})$			
			Tuckerman [20]	**Toh et al. [19]**	**Present numerical results**	**Error (%)**
1	181	4.7	0.110	0.157	0.149	0.35
2	277	6.5	0.133	0.128	0.115	0.13
3	790	8.6	0.090	0.105	0.0958	0.06

5. Optimization

The optimization of PCR to minimize the temperature deviation (T_{dev}) and pressure drop Δp has been conducted to explore the influence of two design variables W_{c} and H_{c},. The optimization problem is defined as:

$$\begin{gathered}\text{Objective function}\\ \min(\mathrm{STD})\ \text{and}\ \min(\Delta P)\\ \text{Subject to: } 150\,\mu\mathrm{m} < W_{\mathrm{c}} < 500\,\mu\mathrm{m}\,;\,50\,\mu\mathrm{m}\\ < H_{\mathrm{c}} < 150\,\mu\mathrm{m}\end{gathered}$$

After choosing the range of the design variables, eighty design of experiments (DOE) points were generated and distributed within design space using D-Optimal design technique. Then, these DOE points were used to provide input parameters for the CFD model implemented in COMSOL Multiphysics® 5.4 which used to determine the corresponding ΔP and, T_{dev} values. MATLAB code was used to create metamodels surfaces based on these CFD results and to build surrogate models using a cubic Radial Basis Functions (RBF) throughout the design space. In the present study, PCR is designed according to the conflicting requirements of minimising temperature deviation T_{dev} and pressure drop ΔP. The T_{dev} with respect to target temperatures at each PCR zones was determined according to the volumetric integral:

$$T_{\mathrm{dev}} = \left(\iiint (T_{fi,j,k} - T_{\mathrm{target}})^2 \mathrm{d}V \right) / \iiint \mathrm{d}V \quad 5$$

The second objective is the Δp which is calculated based on COMSOL results as:

$$\Delta P = P_{\mathrm{in}} - P_{\mathrm{out}} \quad 6$$

where P_{in} and P_{out} represent the pressure at channel inlet and outlet, respectively.

6. Results

The metamodels of ΔP and T_{dev} are depicted in Fig. 3. These show that each objective has a simple dependency on design variables in that that optima lie on design space boundaries. These dependencies are shown more clearly in Fig. 4. It can be noted from Figs. 3 and 4 that it is not possible to move along the design points on the meta-surface to minimize any of the objective functions without increasing at the other objective function.

Fig. 3

Response surfaces of $\Delta p\,(\mathrm{pa})$ and $T_{\mathrm{dev}}\,(\mathrm{K})$ in terms of W_{c} and H_{c} for the PCR

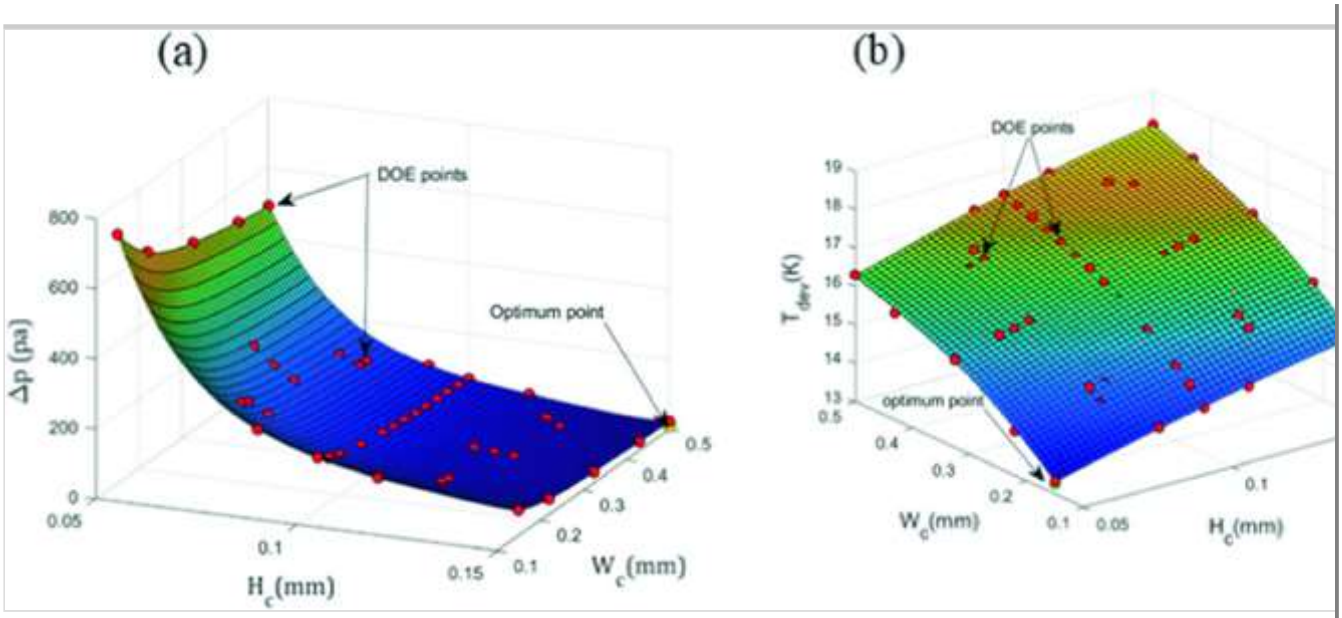

Fig. 4

Global optimization design trend obtained from metamodels

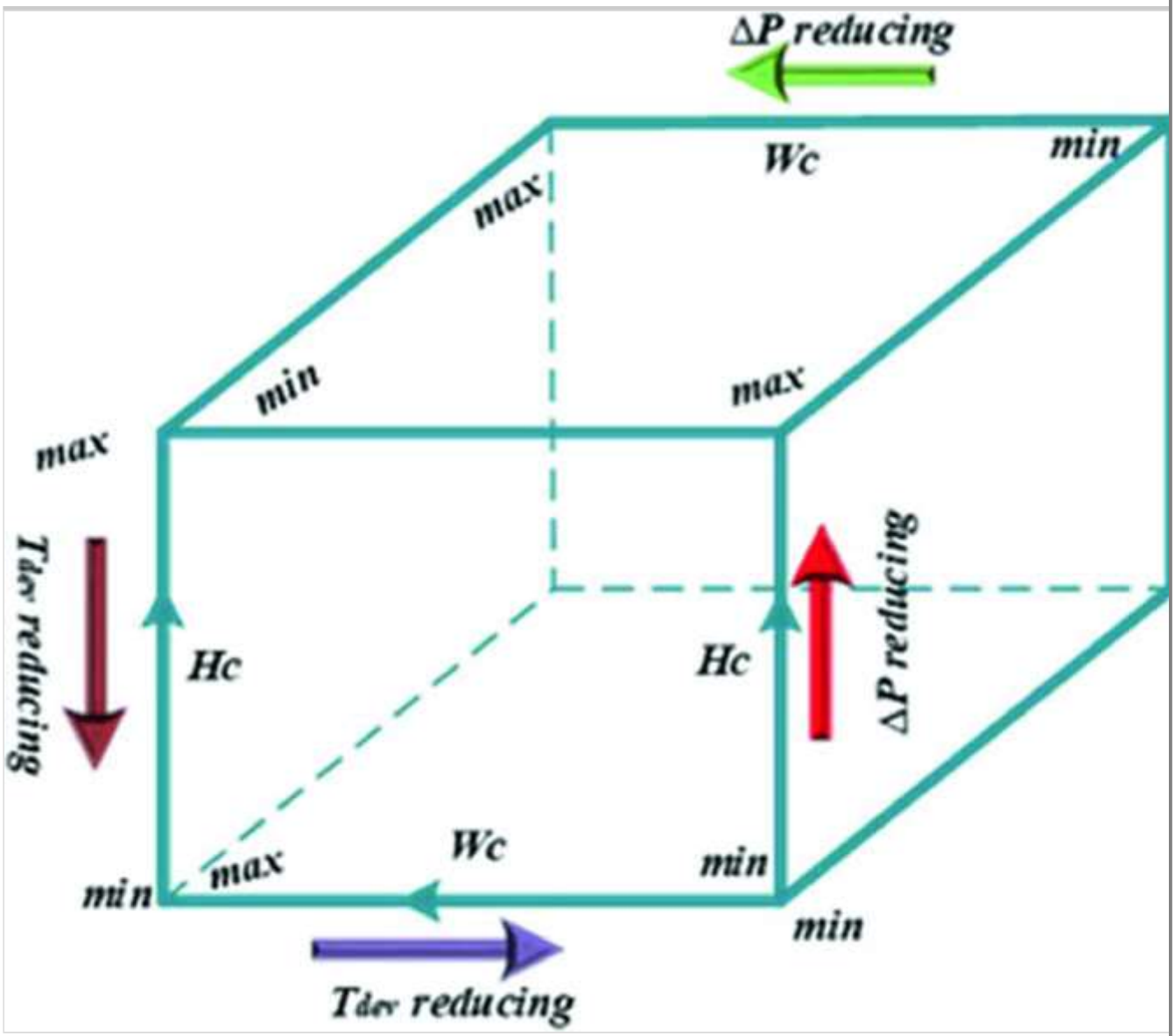

6.1. Single Objective Optimization

The surrogate models are investigated for each objective individually in order to optimize each objective and explorer the competence between them. Figure 3a–b shows the surrogate model surface between ΔP and T_{dev} against W_{c} and H_{c}. Figure 3a shows that minimizing ΔP demand biggest channel size (W_{c} and H_{c}) whereas Fig. 3b illustrates that minimizing the T_{dev} requires smallest channel size (W_{c} and H_{c}). The optimum solution values at each objective are depicted in Table 2 which revels the conflict between the objectives and it is interesting to find the trade-of between the objective functions through a multi-objective analysis.

Table 2

Global optimization

Parameter	Optimum value	Corresponding values			
		Δp (pa)	T_{dev} (K)	W_{c} (mm)	H_{c} (mm)
T_{dev} (K)	13.27	708	–	0.15	0.05
Δp (pa)	23.3	–	17.9	0.5	0.15

7. Conclusion

In this paper, a three-dimensional CFD mathematical model has been solved using COMSOL Multiphysics® 5.4 and coupled with MATLAB optimization code to achieve optimization of PCR systems. Also this work enabled the multi-objective optimization which can be used to improve the thermal performance of CFPCR in terms of temperature deviation, pressure drop, and heating power in microfluidic channels. It can be noted from Fig. 2a–b that when W_{c} increases, the pressure drop decreases, and when H_{c} increases, the pressure drop decreases. Also, the temperature deviation T_{dev} increases with an increase of W_{c} and H_{c} which means that the temperature uniformity decreases. A novel first study focuses on a prototype serpentine microfluidic geometry and a optimization study is determined using accurate meta-modelling and stochastic optimization methods that enabled a series of Pareto fronts to determine

compromises that can be struck between the competing multiple objectives in PCR systems.

Acknowledgements

The authors are grateful to the Ministry of oil, Iraq, and the British petroleum (BP), Iraq, for sponsoring the work on this project.

References

1. A.F. Al-Neama et al., An experimental and numerical investigation of chevron fin structures in serpentine minichannel heat sinks. **120**, 1213–1228 (2018)

2. A.D. Stroock, et al., Chaotic mixer for microchannels **295**(5555), 647–651 (2002)

3. M.D. Tarn, et al., The study of atmospheric ice-nucleating particles via microfluidically generated droplets **22**, 1–25 (2018)

4. J. Chen, K.J.M. Li, Analysis of PCR kinetics inside a microfluidic DNA amplification system **9**(2), 48 (2018)

5. Y.S. Shin, et al., PDMS-based micro PCR chip with parylene coating **13**(5), 768 (2003)

6. C. Zhang, D. Xing, Y.J. B.A. Li, Micropumps, microvalves, and micromixers within PCR microfluidic chips: advances and trends **25**(5), 483–514 (2007)

7. Z. Chunsun et al., Continuous-flow polymerase chain reaction microfluidics based on polytetrafluoethylene capillary. Chin. J. Anal. Chem. **34**(8), 1197–1203 (2006)

8. C.D. Ahrberg, A. Manz, B.G. Chung, Polymerase chain reaction in microfluidic devices. Lab Chip **16**(20), 3866–3884 (2016)

9. M.A. Northrup, DNA amplification with a microfabricated reaction chamber, in *Technical Digest of 7th International Conference on Solid-State Sensors and Actuators* (1993)

10. S. Kumar, T. Thorsen, S.K. Das, Thermal modeling for design optimization of a microfluidic device for continuous flow polymerase chain reaction (PCR), in *ASME 2008 Heat Transfer Summer Conference collocated with the*

Fluids Engineering, Energy Sustainability, and 3rd Energy Nanotechnology Conferences (American Society of Mechanical Engineers, 2008)

11. Y. Zhang, P. Ozdemir, Microfluidic DNA amplification—a review. Anal. Chim. Acta. **638**(2), 115–125 (2009)

12. M.U. Kopp, A.J. De Mello, A. Manz, Chemical amplification: continuous-flow PCR on a chip. Science **280**(5366), 1046–1048 (1998)

13. N. Crews, C. Wittwer, B. Gale, Continuous-flow thermal gradient PCR. Biomed. Microdevice **10**(2), 187–195 (2008)

14. D. Moschou et al., All-plastic, low-power, disposable, continuous-flow PCR chip with integrated microheaters for rapid DNA amplification. Sens. Actuators B: Chem. **199**, 470–478 (2014)

15. I. Schneegaß, R. Bräutigam, J.M. Köhler, Miniaturized flow-through PCR with different template types in a silicon chip thermocycler. Lab Chip **1**(1), 42–49 (2001)

16. M. Hashimoto et al., Rapid PCR in a continuous flow device. Lab Chip **4**(6), 638–645 (2004)

17. Q. Zhang et al., Temperature analysis of continuous-flow micro-PCR based on FEA. Sens. Actuators B: Chem. **82**(1), 75–81 (2002)

18. J.J. Chen, C.M. Shen, Y.W.J.B.M. Ko, Analytical study of a microfludic DNA amplification chip using water cooling effect **15**(2), 261–278 (2013)

19. K. Toh, X. Chen, J. Chai, Numerical computation of fluid flow and heat transfer in microchannels. Int. J. Heat Mass Transf. **45**(26), 5133–5141 (2002)

20. D.B. Tuckerman, *Heat-Transfer Microstructures for Integrated Circuits* (Lawrence Livermore National Lab Ca, 1984)